



Design and simulation of antireflection coating systems for optoelectronic devices: Application to silicon solar cells

D. Bouhafs^{a,*}, A. Moussi^a, A. Chikouche^a, J.M. Ruiz^b

^a *L.C. Photovoltaïques/U.D.T.S., 2, Bd Frantz Fanon, B.P. 399, Alger-Gare, Alger, Algeria*

^b *Instituto de Energia Solar, E.T.S.I. Telecomunicacion, Universidad Politécnic de Madrid, 28040 Madrid, Spain*

Received 4 May 1997

Abstract

Reflectance calculation for various single-, double- and triple-layer *Antireflection* coatings (ARCs) on silicon substrate are presented. A calculation program is developed to determine the optimum thickness and the refractive index of each layer at a single wavelength for optoelectronic applications and through the visible spectrum for photovoltaic applications.

Ta₂O₅, ZnS, Al₂O₃ single layer, MgF₂/ZnS double layer and MgF₂/Al₂O₃/ZnS triple layer ARC systems are deposited on silicon substrate using electron beam and thermal evaporation as deposition techniques. The reflectance as a function of the wavelength of AR coating systems on silicon substrate is measured. All curves show good accordance between the theoretical and the experimental reflectance. As application in the photovoltaic field, a ZnS single-layer AR coating is evaporated on concentrator silicon solar cells. Spectral response and current–voltage characteristics are measured before and after ZnS ARC deposition to estimate the improvement of the cell performances. Short-circuit current and cell efficiency are increased by about 31% and 29.4%, respectively. © 1998 Elsevier Science B.V. All rights reserved.

Keywords: Antireflection coating; Optoelectronic devices; Silicon solar cells

1. Introduction

It is well known that the application of one or more antireflection coating layer on the front surface of the photovoltaic cells and optoelectronic devices (Lasers, IR

* Corresponding author.

diodes, etc) reduces the amount of reflection of the incident light, which improves the device performance [1–5]. Kern and Tracy [6] have observed an increase of about 44% of the cell efficiency after spraying TiO_2 single-layer ARC. Green et al. [7] have used MgF_2/ZnS two-layers on silicon cells with 19.1% efficiency. The use, for silicon solar cells, of more than two layers ARCs in practice is limited.

The theory of antireflection coating is examined by many authors [8–11] for determining the optimum thickness and materials to be used as ARCs on polished or textured silicon. The matrix method [11] is usually employed for calculation of reflection coefficient.

In this paper, we present the result of calculations obtained by our computer programme of one-, two- and three-layer ARCs on silicon substrate. Theoretical results are shown in Section 1

The process of the cell fabrication is presented in Section 2. In Section 3 we give the experimental measurements of optical and electrical characterisation and discussion about these results.

2. Theory

Direct matrix method is used to evaluate the reflection coefficient of a multilayer system on silicon substrate. The system of N layers, Fig. 1, is characterised by the equivalent matrix M_{eq} , which relates the amplitudes of electromagnetic field components at the (N th) interface with the incident electromagnetic field components.

The equivalent matrix of N layers interlocked between two semi-infinite mediums is given in Ref. [12]

$$M_{\text{eq}} = \prod_{j=1}^{j=N} \begin{pmatrix} \cos \varphi_j & (i/n_j^{\text{eff}}) \sin \varphi_j \\ in_j^{\text{eff}} \sin \varphi_j & \cos \varphi_j \end{pmatrix} \quad (1)$$

where $i^2 = -1$, n_j is the refractive index of j th layer, φ_j is the phase thickness of j th layer, $\varphi_j = 2\pi/\lambda n_j^{\text{eff}} d_j$, $n_j^{\text{eff}} = n_j \cos \theta_j$ for parallel polarisation, $n_j^{\text{eff}} = n_j / \cos \theta_j$ for

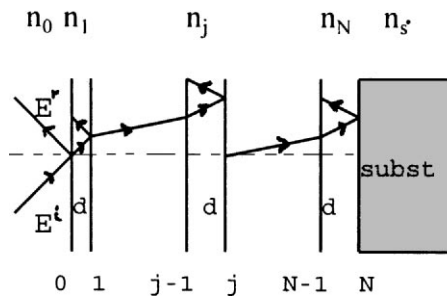


Fig. 1. A multilayer stack scheme of N layers on a semi-infinite substrate n_s .

perpendicular polarisation and θ_j is the incident angle in the layer j . It is calculated from the Snell's law:

$$n_{j-1} \sin \theta_{j-1} = n_j \sin \theta_j$$

Many different types of optoelectronic devices such as LASER and IR photo-diodes need a very low reflectance at a defined wavelength (λ) [13]. The antireflection coating system (one layer or more) for each application are calculated for a minimum reflectance $R(\lambda)$. Analytical or contour methods are generally used to determine the optimum parameters (n , d) of the optical films.

For photovoltaic cells it is important to have a minimum reflection over all the visible spectrum (300–1100 nm). The cell performance is influenced by other parameters such as the photon flux $F(\lambda)$ and the cell internal quantum efficiency $Q_i(\lambda)$ [1,8]. Since the reflection coefficient needs to be minimised where $F(\lambda)$ and $Q_i(\lambda)$ have their maximum values, the weighted reflectance R_w is calculated from Ref. [8]:

$$R_w = \frac{\int_{\lambda_1}^{\lambda_2} F_i(\lambda) Q_i(\lambda) R(\lambda) d\lambda}{\int_{\lambda_1}^{\lambda_2} F_i(\lambda) Q_i(\lambda) d\lambda}. \quad (2)$$

Silicon substrate is considered absorptive and the dispersion law is taken into account using data from Refs. [14,15]. Materials used as ARCs are assumed to be transparent. Values of $F(\lambda)$ and $Q_i(\lambda)$ used in the programme are extracted from [16,17] corresponding to the AM 1.5 solar spectrum.

Various methods have been used for the design of a multilayer optical thin film system [18–20]. In this case, the contour method [17,22] is used for determining the optimal parameters.

The refractive index n and thickness d are determined with the minimal weighted reflectance R_w .

2.1. Single-layer ARC

2.1.1. Single wavelength

In some applications (Laser, photodiodes etc.) zero reflectance is needed at a single wavelength or throughout a narrow spectrum band. For determining the optimum thickness and refractive index with a minimum reflectance, the following equations are deduced from Eq. (1):

$$n = (n_0 n_s - (n_0 k_s)/(n_0 - n_s))^{1/2}, \quad (3)$$

$$d = (\lambda/2\pi) \arctg ([n_0(n_0 - n_s)/(n_0 k_s)], \quad (4)$$

where n_0 is the refractive index of the incident medium, n_s the refractive index of the substrate and k_s the extinction coefficient of the substrate. For each wavelength we have to calculate n and d which give $R(\lambda) = 0$ from Eqs. (3) and (4), respectively. Fig. 2 shows the curves of the optimum values of n and d .

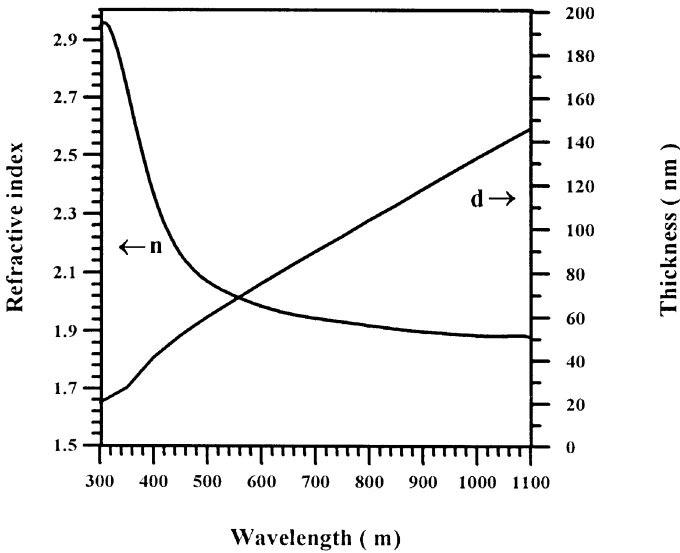


Fig. 2. Optimum values of (n,d) pairs vs. wavelength for a single antireflection coating on silicon. Each pair (n,d) gives zero reflection at a defined wavelength.

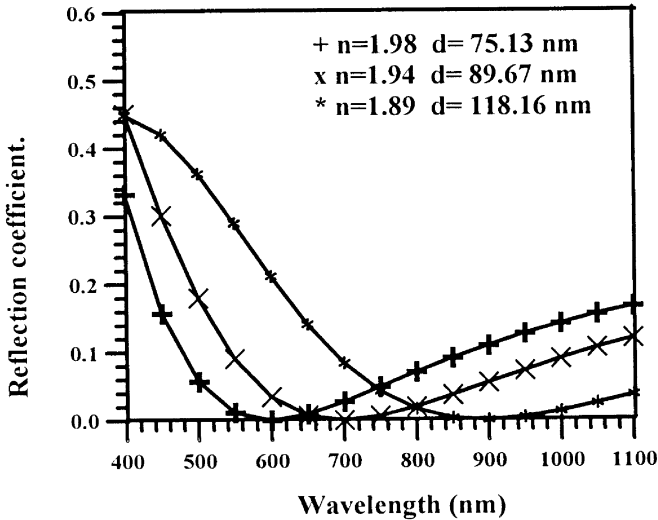


Fig. 3. Reflectance spectra vs. wavelength for some optimised single-layer antireflection coating on silicon.

Fig. 3 illustrates the reflectance spectra of three optimised single-layer ARC systems on silicon substrate. For a lower value of n , a higher corresponding value of d is obtained (Eqs. (3) and (4)) and we show that the minimum reflectance is shifted to the long-wavelength spectral region (Fig. 3).

2.1.2. UV-visible spectrum

Weighted reflectance are calculated from Eq. (2) for determining the optimum values of n and d with R_w minimum. Results are illustrated in Fig. 4. The lowest value $R_w - 6.2\%$ is obtained with $n = 1.96, d = 86$ nm. This value $n = 1.96$ can correspond to the TiO_x deposited by spray [6] or to CeO by vacuum evaporation [2]. Taking into account experimental data [1,2,6] of materials used usually as AR coatings we have calculated some single-layer ARCs for silicon solar cells. From Table 1 we show that the minimum of R_w is higher than the optimised value due to fluctuation of the refractive index.

2.2. Two-layer ARCs

2.2.1. Single wavelength

The Schuster diagram [21] for silicon substrate is established to choose the optimum index of the inner and outer layers. A diagram in which n_2 , the refractive index of the inner layer is plotted against n_1 , the refractive index of the outer layer. It illustrates the conditions which give a zero reflection:

$$AB/CD > 0$$

where

$$A = n_0 - n_s, \quad B = n_0 n_2^2 - n_1^2 n_s,$$

$$C = n_0 n_s - n_2^2, \quad D = n_1^2 - n_0 n_s,$$

For more details, Ref. [21] gives explicitly the different steps of calculations.

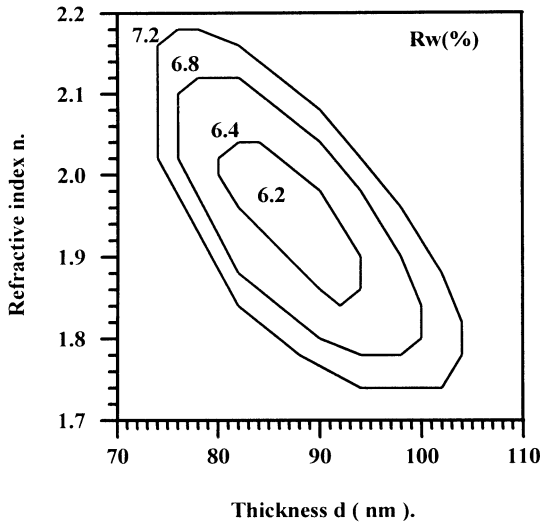


Fig. 4. Contours of weighted reflectance for a single-layer AR coating on silicon as a function of thickness and refractive index.

Table 1
Optimised single-layer AR coating on polished silicon substrate

Material	TiO ₂ (Spray)	Ta ₂ O ₅	ZnS	SiO ₂
Refractive index (n)	2.0	2.1	2.3	1.46
Thickness d (nm)	82.0	80.0	68	110
Weighted reflectance R_w %	8.9	9	10.7	11.77

The design with low-high index on silicon substrate in which the outer layer has the low refractive index and the inner layer has high refractive index is used. This choice is based on the spectral stability of the coating and for low reflectance. Stability means that the low-reflectance spectrum changes very slightly with thickness and refractive index variations. Generally, the experimental conditions affect the thickness and refractive index values of the deposited layer and, consequently, the desired low reflectance value. Calculations show that the L–H design gives more advantage than the H–L design to keep the low reflectance value with the variations of n and d of each layer in the ARC system during deposition. The most stable coatings are those which have an inner layer whose refractive index is close to that of the substrate and the outer layer whose refractive index is close to that of the incident medium [23].

Fig. 5 shows the contours of equal reflectance $R(\lambda)$ plotted against the thickness of both layers at $\lambda = 600$ nm. The minimum reflectance obtained is 1×10^{-4} (%) with $d_1 = 55.5$ nm and $d_2 = 53.2$ nm. The corresponding reflectance spectra of the optimised AR coating system are shown in Fig. 6. One minimum appears at $\lambda = 600$ nm. Such AR coating systems are used in photodiodes (LASER) and other optoelectronic devices which need a minimum reflectance spectra of the optimised AR coating system are shown in Fig. 6. One minimum appears at $\lambda = 600$ nm. Such AR coating systems are used in photodiodes (LASER) and other optoelectronic devices which need a minimum reflectance at a single wavelength.

2.2.2. UV-visible spectrum

For photovoltaic applications the reflectance is minimised through the visible spectrum.

Fig. 7 shows the R_w contours in which appear the low value $R_w = 2.39\%$ obtained with $n_1 = 1.4$, $n_2 = 2.5$, $d_1 = 11.5$ nm, $d_2 = 65$ nm. Table 2 illustrates the results of the calculated ARC systems with several existing materials such as MgF₂, SiO₂, Ta₂O₅ and ZnS.

The refractive index values $n_1 = 1.4$, $n_2 = 2.5$ correspond to MgF₂ and TiO₂ deposited by evaporation techniques, respectively. We show (Table 2) that a lower fluctuation in n_2 causes a variation in the weighted reflectance coefficient R_w . This variation aided the optimum choice of the technological parameters of the technique to reduce the fluctuation commonly appearing during the deposition.

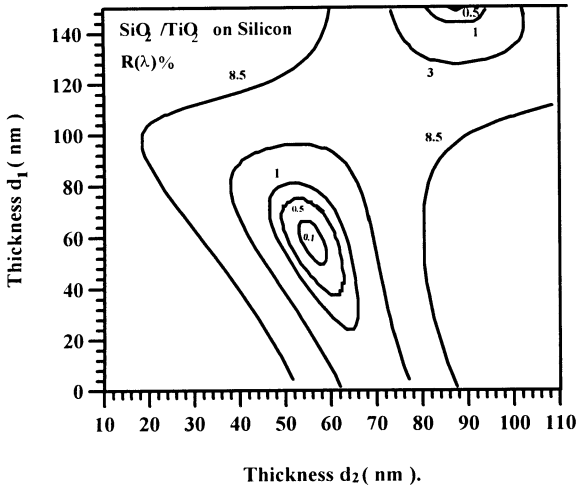


Fig. 5. Contours of weighted reflectance of SiO₂/TiO₂ ARCs plotted against d_{SiO_2} and d_{TiO_2} at $\lambda = 600$ nm.

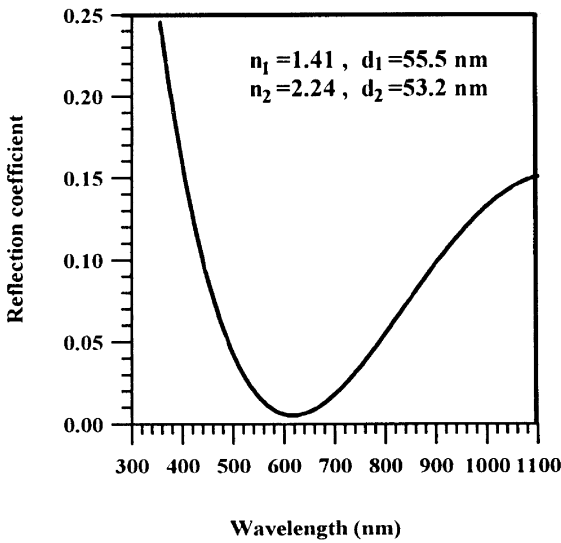


Fig. 6. Reflectance spectra vs. wavelength for SiO₂/TiO₂ two-layer ARCs on silicon substrate. $R_{\text{min}}(\lambda) = 1 \times 10^{-4}$ (%) at $\lambda = 600$ nm.

2.3. Three-layer ARCs

The design of three-layer ARCs on silicon is optimised using Eq. (2) when the optimum refractive index of each layer in the stack is calculated by [5]:

$$n_2^2 = n_0 \cdot n_s = n_1 \cdot n_3,$$

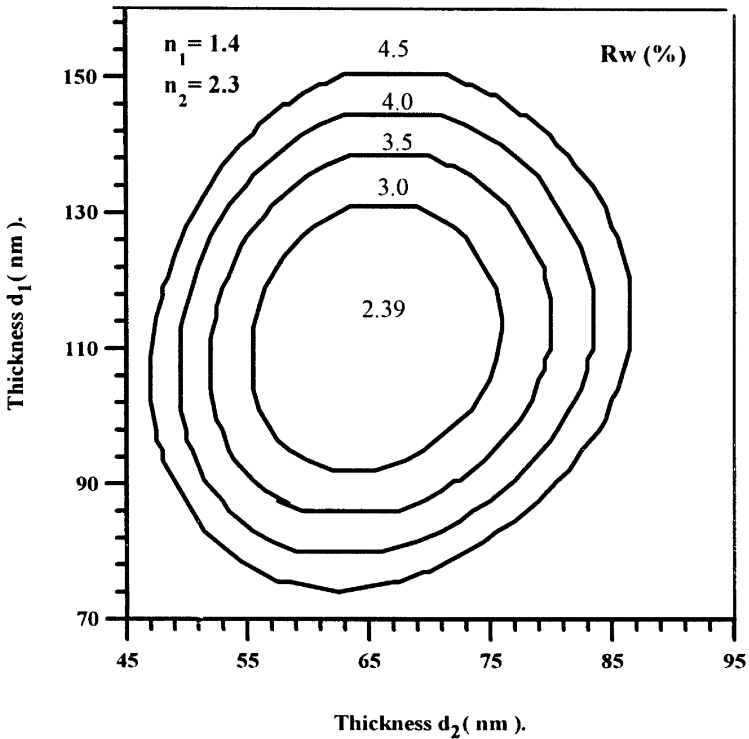


Fig. 7. Contours of weighted reflectance for two-layer ARCs on silicon as a function of the inner and the outer layer thickness (d_1, d_2).

Table 2

Optimum parameters of some two-layer AR coatings design on polished silicon substrate

System (L, H)	n_1	n_2	$d_1(\text{nm})$	$d_2(\text{nm})$	$R_w(\%)$
(1.41, 2.24)	1.41	2.24	112.0	69.0	2.65
(1.5, 2.0)	1.50	2.00	072.5	60.0	6.23
(1.5, 2.1)	1.50	2.10	071.5	61.0	6.25
(1.5, 2.5)	1.50	2.50	098.0	61.5	2.98
(1.4, 2.0)	1.40	2.00	93.5	70.0	5.32
(1.4, 2.1)	1.40	2.10	078.5	68.5	4.77
(1.4, 2.5)	1.40	2.5	111.5	65.0	2.39

where n_2 is the refractive index of the medium layer. The refractive index decreases from the high value (n_s) to the low value ($n_{\text{air}} = 1$) in the order: $n_{\text{air}} < n_1 < n_2 < n_3 < n_s$.

Table 3 shows the optimum values. We note that it is not possible to deposit materials with a refractive index $n = 2.78$ which does not absorb an appreciable

Table 3
Optimum parameters of three-layer AR coatings design on polished silicon substrate

AR coating design	Layer parameters	Outer layer	Medium layer	Inner layer
Optimum calculated design	Refractive index	1.40	1.97	2.78
	Thickness $d(\text{nm})$	104	55	51
	Weighted reflectance $R_w(\%)$		1.4	
Calculated design with practical materials	Refractive index	1.38	1.63	2.3
	Thickness $d(\text{nm})$	82	33	54
	Weighted reflectance $R_w(\%)$		2.4	

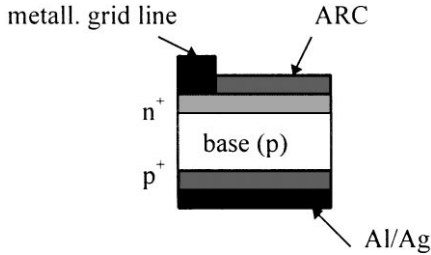


Fig. 8. n^+pp^+ silicon solar cell structure with antireflection coating.

amount of the incident light [2]. Using materials deposited by vacuum evaporation such as ZnS ($n = 2.3\text{--}2.4$), Al_2O_3 ($n = 1.63$) and MgF_2 ($n = 1.38$), three-layer ARC systems on silicon are calculated. Table 3 shows that $R_w = 2.4\%$ is higher than the minimal value $R_w = 1.4\%$ obtained with the optimum system.

3. Experimental procedure

n^+pp^+ silicon solar cells are fabricated using a $4\text{--}5\ \Omega\text{cm}$ boron-doped single-crystal silicon wafers. Emitter region n^+ are realised by diffusing phosphorous atoms from a POCl_3 liquid source. p^+ region (BSF) are formed by evaporating a thin layer of aluminium on the rear surface. Drive-in of P and Al atoms was carried in a quartz tube furnace simultaneously at 850°C . Ti/Pd/Ag grid metallisation are evaporated on the front surface. The cell rear contact is realised by deposition of a thin layer of Al/Ag, Fig. 8. Before AR coating, deposition cell performances are characterised at standard conditions (AM 1.5, 25°C).

One-, two- and three-layer ARCs are deposited on silicon substrates in a stainless steel bell jar from a thermal tungsten crucible for ZnS and by an electron gun for MgF_2 , Ta_2O_5 , Al_2O_3 using a cleaned C and Mo crucibles. Pressure reached in deposit chamber is $10^{-5}\text{--}10^{-6}$ torr. The deposition rate and the thickness of the films are controlled in situ by a quartz crystal monitor through an SCT200 processor from SYCON Instruments.

Reflectance spectra was measured in the range 400–1100 nm by a Spectro320 Instrument Systems GmbH spectrophotometer.

Current–voltage characteristic (I – V) and spectral response are measured for a silicon solar cell with ZnS ARC to estimate the improvement in the cell's performance after ARC deposition. Electrical characterisation are done at the ISPRA Laboratory, (Varese, Italy).

4. Experimental results and discussion

Optical measurements of the reflectance spectra of Ta₂O₅ ARC layer deposited on silicon are shown in Fig. 9. A minimum value of reflectance $R(\lambda) = 0.1\%$ is obtained at 650 nm. Good agreement is observed between the experimental and calculated reflectance spectra. The refractive index and thickness used in the calculations are 2.1 and 80 nm, respectively. The difference observed in the short- and the long-wavelength regions is due to the dispersion of the Ta₂O₅ refractive index.

The reflectance spectra of the ZnS ARC evaporated on silicon are shown in Fig. 10. Good accordance is seen between the experimental and the calculated $R(\lambda)$ curve throughout the visible spectrum. We note that the ZnS layer is more transparent in the short wavelength region ($\lambda \leq 500$ nm) than the Ta₂O₅ layer (Fig. 9). I – V characteristic and spectral response of the cells indicate a good transparency of the ZnS layer in the short wavelength region. The absorption of the Ta₂O₅ is attributed to the presence of excess free oxygen atoms in the deposited film, due probably to the dissociation of the Ta₂O₅ molecules during electron beam evaporation.

Fig. 11 shows reflectance curve of MgF₂/ZnS two-layer ARC on which appear two minima: the first $R_{\min 1} = 9.1\%$ at 500 nm, the second $R_{\min 2} = 0.58\%$ at 1000 nm. The

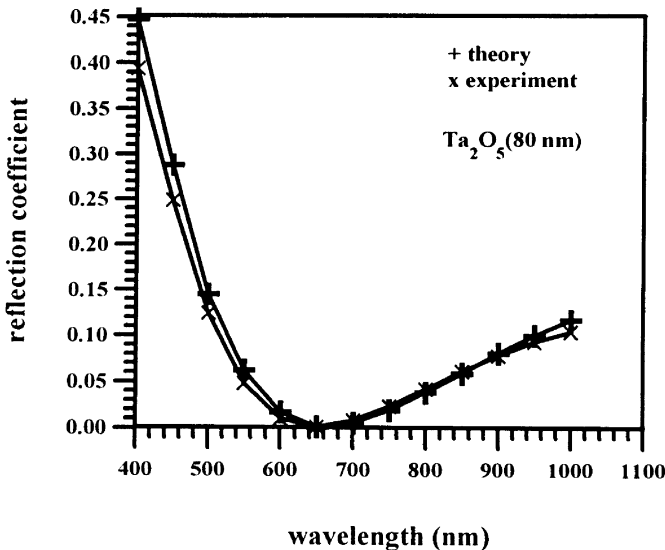


Fig. 9. Measured and calculated reflectance of Ta₂O₅ ARC on silicon.

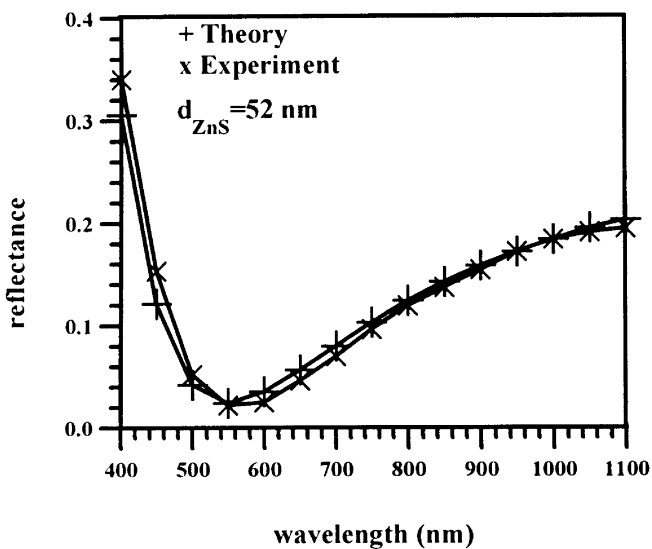


Fig. 10. Measured and calculated spectral reflectance of ZnS ARC on silicon.

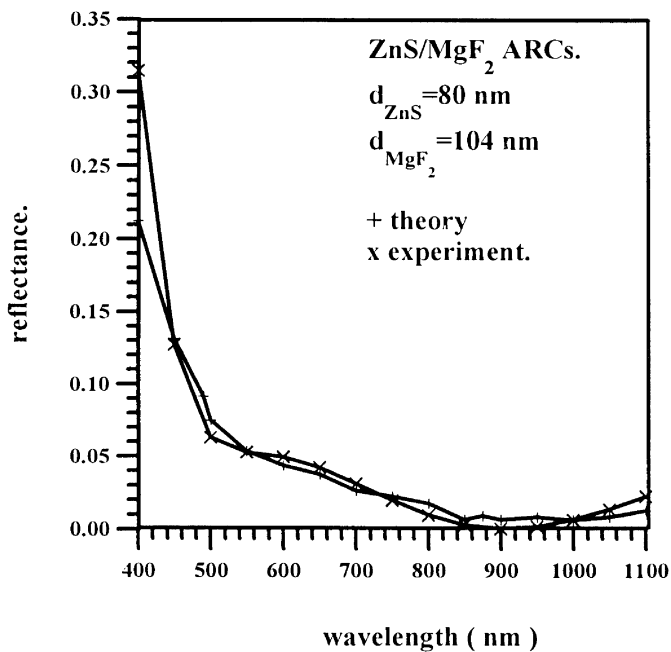


Fig. 11. Experimental and calculated reflectance vs. wavelength of MgF₂/ZnS two-layer ARC on silicon.

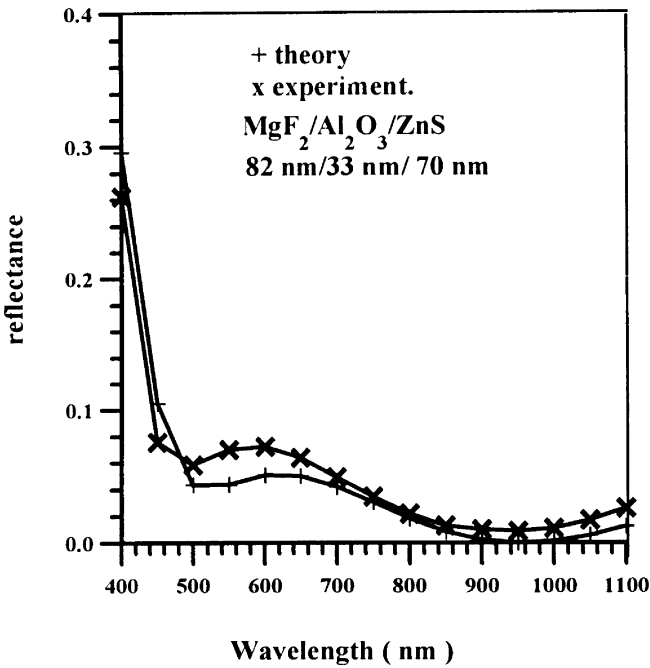


Fig. 12. Measured and calculated spectral reflectance of MgF₂/Al₂O₃/ZnS triple-layer ARCs on silicon.

reflectance $R(\lambda)$ is lower than 3% in the range $720 \text{ nm} \leq \lambda \leq 1100 \text{ nm}$ which maximises the absorption of the incident photons and increases the photo-generated current. On the basis of theoretical calculations [1,24], the reflectance value in the short wavelength region is affected by the outer layer (MgF₂) thickness for which the deposited thickness is estimated to be lower than the needed value (optimum).

Fig. 12 shows the experimental reflectance of the MgF₂/Al₂O₃/ZnS three-layers on silicon. Two minima appear; $R_{\min 1} = 5.8\%$ at $\lambda = 500 \text{ nm}$, $R_{\min 2} = 0.88\%$ at $\lambda = 1000 \text{ nm}$. Through the range 800–1100 nm the reflectance is lower than 3%. The curve $R(\lambda)$ (Fig. 12) is characterised by a broader low reflectance. Good accordance is observed between the calculated and the experimental curves. The difference in the short wavelength region is probably due to the dispersion of the refractive index in the wavelength region.

Fig. 13 gives the current–voltage characteristics. It shows the improvement of the short-circuit current and efficiency after ZnS and Ta₂O₅ AR coating deposition. The I – V characteristic with a ZnS AR coating is better than that with Ta₂O₅ ARC. Table 4 shows the cell's performance before and after ZnS AR coating. The short-circuit current and the cell efficiency show an increase of about 31% and 29.4% respectively. The open-circuit voltage V_{oc} and the fill factor FF are not influenced by the ARC deposition; the slight variation observed could be attributed to the circuit measurement error.

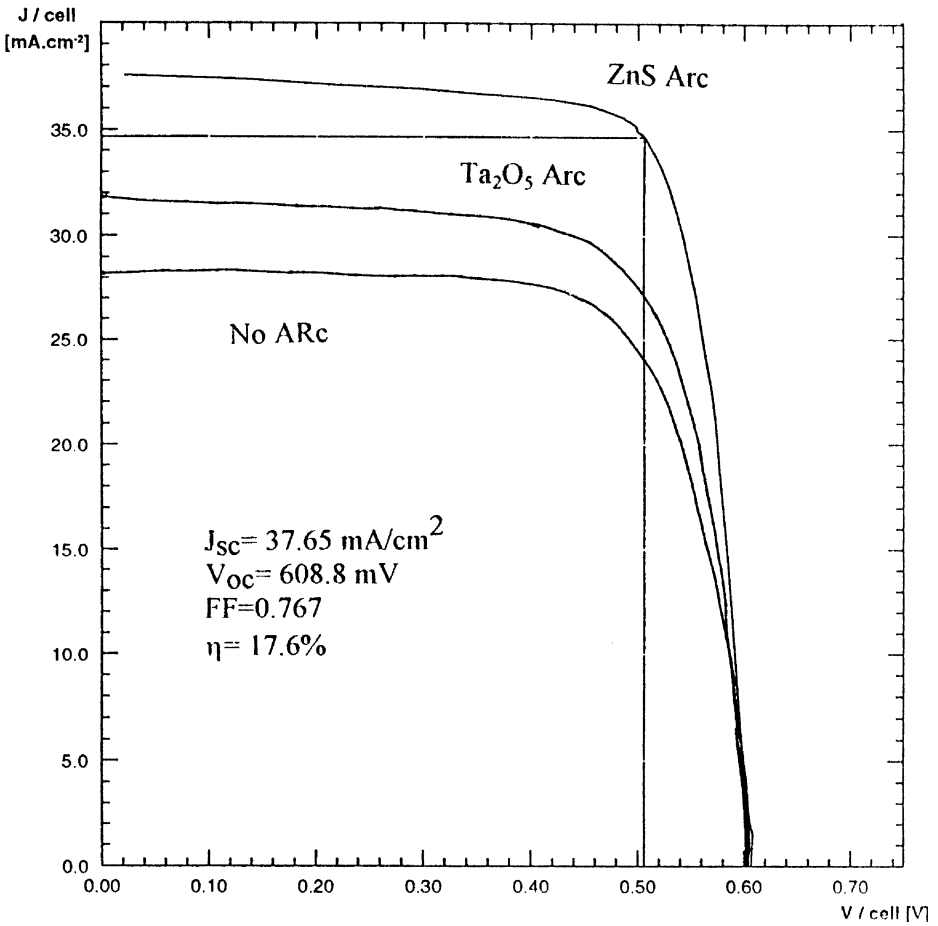


Fig. 13. Silicon solar cell $I-V$ characteristics before and after ZnS ($d = 52 \text{ nm}$) and Ta_2O_5 (80 nm) single-layer antireflection coating.

Table 4
Cell's performance before and after ZnS coating

	J_{sc} (mA/cm ²)	FF (%)	V_{oc} (mV)	$\eta\%$
No AR coating	28.3	0.79	607.0	13.6
With ZnS AR coating	37.1	0.767	608.3	17.6

We give Fig. 14 the spectral response $Sr(\lambda)$ of the cell before and after a ZnS ARC deposition. The $Sr(\lambda)$ is increased uniformly throughout the spectrum range. The curve shows a maximum in the long-wavelength region due to the back-surface field effect which reduces the recombination at the back side, therefore, decrease of the

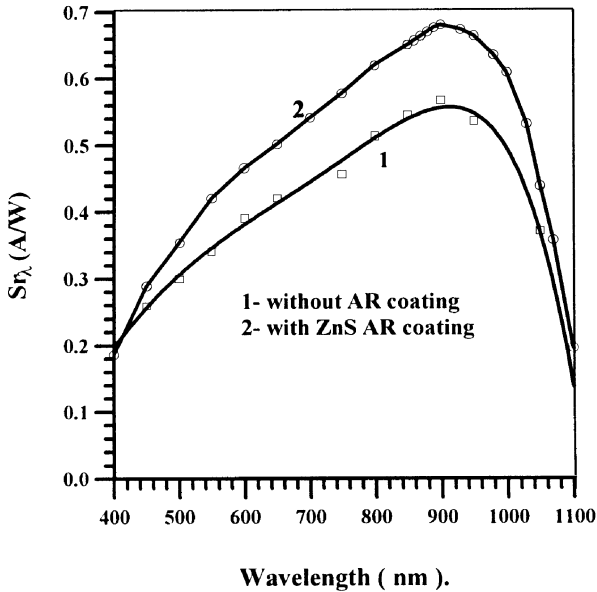


Fig. 14. Spectral response of silicon solar cell. (1) without AR coating; (2) with a ZnS single-layer AR coating ($d = 52$ nm).

diode leakage current [25] and increase of the collection efficiency of the minority carries generated by the NIR photons.

5. Conclusions

A theoretical study of the antireflection coatings on silicon solar cells is made. A model programme is developed for the best design of antireflection coating for an arbitrary substrate n_s and incident angle of light. Polished and textured silicon surfaces are taken into account. Our developed simulator can be used also for the optimisation of AR coating for optoelectronic devices to improve the power output parameters.

One-, two- and three-layer ARCs on silicon are calculated at normal incidence. The optimum refractive index and thickness are determined. Ta_2O_5 , ZnS single-layer, MgF_2/ZnS two-layer and $MgF_2/Al_2O_3/ZnS$ three-layer antireflection coatings are deposited by thermal and electron beam evaporation on silicon.

Reflectance spectra of deposited ARC layers on silicon are measured. The theoretical and experimental $R(\lambda)$ curves present a good accordance. Current–voltage characteristic and spectral response for a silicon solar cell with a ZnS ARC show an amelioration after antireflection deposition. Fill factor and open-circuit voltage are weakly influenced by the antireflection coating deposition.

Acknowledgements

This work was supported by the Unité de Développement de la Technologie du Silicium/Ministère de l'Enseignement Supérieur et de la Recherche Scientifique, Alger, and in part realised in the Instituto de Energia Solar, Madrid.

References

- [1] G.E. Jellison Jr., R.F. Wood, *Solar Cells* 18 (1986) 93.
- [2] J. Zhao, M.A. Green, *IEEE Trans. on Electronic Dev.* 38 (8), 1991.
- [3] P.A. Iles, *J. Vac. Sci. Technol.* 14 (1977) 1100.
- [4] P.A. Young, W.G. Thege, *J. Phys. D: Appl. Phys.* 4 (1971) 64.
- [5] J. Thomas Cox, Georg Hass, Antireflection coatings for optical and infrared optical materials, in: *Physics of Thin Films Collec.*, vol. 2, Academic Press, New York, 1964.
- [6] W. Kern, E. Tracy, *RCA Review* 41 (1980) 133.
- [7] M.A. Green et al., *Appl. Phys. Lett.* 44 (1984) 1163.
- [8] D. Redfield, *Solar Cells* 3 (1981) 27.
- [9] B.L. Sopori, R.A. Pryor, *Solar Cells* 8 (1983) 249.
- [10] B. Gandham, et al., *Solar Cells* 1 (1979/1980) 3.
- [11] P.H. Berning, Theory and calculation of optical thin films, in: *Physics of Thin Films Collec.*, vol. 1, Academic Press, New York, 1963, p. 69.
- [12] J. Mouchart, *Appl. Optics* 16 (9) (1977).
- [13] K. Rabinovitch, A. Pagis, *Appl. Optics* 14 (5) (1975).
- [14] G.E. Jellison, F.A. Modine, *J. Appl. Phys.* 53 (1982) 3745.
- [15] Ed. Palik, *Handbook of optical constants of solids*, Academic Press, New York, 1985.
- [16] R.H. Bube, *Fundamental of solar cells*, Academic Press, New York, 1983.
- [17] R.B. Pettit, C.J. Brinker, C.S. Ashley, *Solar Cells* 15 (1985) 267.
- [18] G. Castagno, F. Demichelis, E. Minetti-Mezzeti, *Appl. Optics* 19 (3) (1980).
- [19] L. Bloom, *Appl. Optics* 20 (1) (1981).
- [20] J.A. Dobrowolski, S.H.C. Piotrowski, *Appl. Optics* 21 (8) (1982).
- [21] B.A. Moys, *Thin Solid Films* 21 (1974) 145.
- [22] M.E. Nell et al., 10th European Photovoltaic Solar Energy Conf., 8–12 April, Lisbon, 1991.
- [23] J.C. Monga, Some concepts for the design of grazing incidence antireflection coating, Science Report, Bhabha Atomic Research Center, Bombay, India, 1992.
- [24] D. Bouhafs, These de magister, L.C.P./U.D.T.S. Alger, 1993.
- [25] K.L. Jiao, W.A. Anderson, *Solar Cells* 22 (1987) 229.